

13. Hougen, O. A., and F. W. Dodge, "The Drying of Gases," p. 14, Edwards Brothers, Inc., Ann Arbor, Mich. (1947).
14. Jury, S. H., J. Franklin Institute, in press.
15. ———, and H. R. Edwards, *Can. J. Chem. Engr.*, in press.
16. ———, to be published.
17. Jury, S. H., and J. S. Horng, to be published.
18. *Ibid.*
19. Jury, S. H., and W. Licht, *Ind. Eng. Chem.*, **44**, 591 (1952).
20. Kelly, K. K., J. C. Southard, and C. T. Anderson, *U.S. Bur. Mines Tech. Papers* 625, 1-73 (1941).
21. Langmuir, I., *J. Am. Chem. Soc.*, **40**, 1361 (1918).
22. Lee, R. G., and T. W. Weber, *Can. J. Chem. Engr.*, **47**, 54 (1969).
23. Lescoeur, H., *Ann. Chem. Phys.*, **21**, 511 (1890).
24. Leung, P. K., and D. Quon, *Can. J. Chem. Engr.*, **44**, 26 (1966).
25. Meyer, O. A., and T. W. Weber, *AIChE J.*, **13**, 457 (1967).
26. Polanyi, M., *Verhandl. Deut. Physik Ges.*, **16**, 1012 (1914).
27. *Ibid.*, **15**, 55 (1916).
28. Powell, D. A., *Nature*, **182**, 792 (1958).
29. Rabinowitch, E., and W. C. Wood, *Trans. Faraday Soc.*, **32**, 947 (1936).
30. Razouk, R. I., A. S. Salem, and R. S. Mikhail, *J. Phys. Chem.*, **64**, 1350 (1960).
31. Van't Hoff, J. H., E. F. Armstrong, W. Hinrichsen, F. Weigert, and G. Just, *Z. Physik. Chem.: Stochiometrie Verwandtschaftslehre*, **45**, Leipzig (1903).
32. Washburn, E. W., ed., "International Critical Tables of Numerical Data, Physics, Chemistry, and Technology," Vol. VII, pp. 295-296, McGraw-Hill, New York (1930).
33. Weiser, H. B., W. A. Milligan, and W. C. Ekholm, *J. Am. Chem. Soc.*, **58**, 1261 (1936).

*Manuscript received March 8, 1971; revision received June 14, 1971; paper accepted June 17, 1971.*

# Flow Attachment to Solid Surfaces: The Coanda Effect

T. PANITZ and D. T. WASAN

Department of Chemical Engineering  
Illinois Institute of Technology, Chicago, Illinois 60616

The phenomenon of flow attachment to solid surfaces, occurring with both liquids and gases, is the long-known though inadequately understood Coanda effect.

A flow visualization study was made using a birefringent milling yellow dye solution flowing over a deflection surface consisting of flat plates. A two-dimensional flow channel with transparent side walls was used. Photographic observations of the development of the Coanda effect reveal the method of flow attachment and confirm a number of literature predictions. One of the most interesting of these phenomena is the existence of a well defined mixing region along the deflection surface.

A simplified model of the flow field has been proposed in order to describe the mechanism governing the Coanda effect. The model is supported by experimental data consisting of pressure profiles obtained along the deflection surface and secondary flow entrainment measurements.

Place a cube of salt in a beaker of water and slowly dissolve it by pouring a stream of water over it. As the salt dissolves, a horizontal surface, instead of the expected irregularly shaped surface, is maintained along the top of the cube. Pour a cup of tea out of a teapot spout. The tea will often flow down the spout and even flow up the underside of the teapot before becoming detached. If the pouring angle from the horizontal is increased, the liquid stream partially adheres and partially detaches itself from the spout. When the teapot is tilted still further, the entire stream detaches completely but the downward jet follows an unexpected diversion from the vertical in that it bends towards the spout. Finally, upon tilting the teapot lower yet and thereby increasing the flow again the expected ballistic curve flow path is obtained.

An extensive qualitative investigation by the noted

rheologist Marcus Reiner (18) points up the occurrence of these and similar effects. Having noticed the flow attachment of fluids to surfaces against the pull of gravity, Reiner and Block (18) designed several experiments to show that adhesion as a surface-tension property can be excluded as an explanation of the effect.

It is well known that if a stream of air is blown through a nozzle slit it will be deflected along the external portion of the nozzle and that it entrains several times the amount of air in the original jet. Furthermore, the pressure along the nozzle surface is much less than atmospheric. This has been called the Coanda effect (2).

The Coanda effect has potential applications in the areas of water purification (U.S. Pat. 2,761,292 and 2,803,591), liquid atomizers (U.S. Pat. 2,713,510 and 2,826,454), spraying devices (U.S. Pat. 2,988,303), moving devices (U.S. Pat. 2,920,448), and smoke control (U.S. Pat. 2,173,550 and 2,187,342). The cooling effect of a Coanda pump makes it feasible for the pumping of cryo-

Correspondence concerning this paper should be addressed to D. T. Wasan.

genic fluids where temperature is a critical factor (17). The high degree of turbulence and mixing make Coanda devices very attractive as burners and combustion devices (U.S. Pat. 2,907,557). The Coanda effect is being used in hydraulic computers and in the control field of fluidics where boundary layer control is important (U.S. Pat. 2,939,650).

Many investigators have published articles on the Coanda effect. In most cases they were concerned with how to make Coanda devices work efficiently, but few have performed experiments to uncover why or how these devices work. Some authors have summarized the important geometrical parameters of Coanda nozzles and obtained data using air as the fluid medium (1, 4, 8-11, 22-24). Others have presented mathematical analyses (3, 7, 12, 16, 20, 21, 25, 26) to explain the phenomenon of flow attachment to curved surfaces. However, no quantitative data or analysis has been reported to date on systems using liquids.

We have in the Coanda type flow a phenomenon which may have far reaching consequences in many chemical engineering processes such as distillation, liquid extraction and gas absorption or desorption, as well as in liquid-solid processes where fluids are contacted over solid packings and mixed, often at very high velocities. An elucidation of the flow mechanism governing the Coanda effect is of primary importance for further characterization and mathematical modelling of the phenomenon. Furthermore, a better understanding of the Coanda effect will invariably lead to the design of contacting devices which will provide more efficient contacting and mixing by taking full advantage of the entrainment properties realized in the Coanda type flow (14).

This paper presents the results of an experimental study which involved the design of an apparatus for flow visualization studies of the Coanda effect using water and a milling yellow dye solution. The study was undertaken to obtain photographic observations and experimental data regarding flow entrainment, the effect of primary jet velocities and the viscosity of the fluids on the adherence of a jet or a jet sheet to a solid surface. Presented in this paper are the results of the first phase of the work which focuses on pressure profiles and secondary flow entrainment measurements.

## APPARATUS AND EXPERIMENTAL PROCEDURE

The experimental apparatus shown in Figure 1 was used to obtain qualitative photographic data and quantitative secondary entrainment and pressure profile data on a Coanda nozzle.

The apparatus consists of a large reservoir (A) which is used for storing the water or milling yellow dye solution and provid-

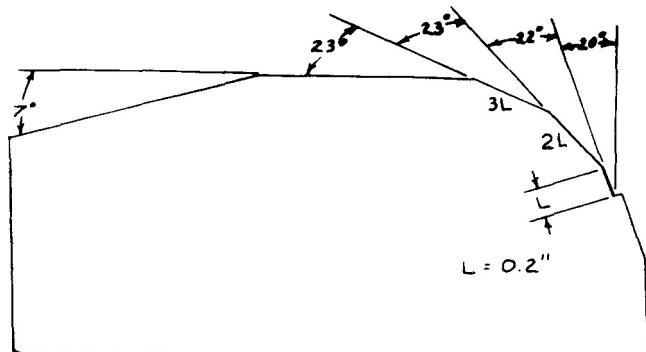


Fig. 2. Dimensions of the Coanda deflection surface.

ing an infinite sink effect for the secondary flow. The flow channel (B) extends from a plexiglass window in the reservoir. The channel consists of a copper plate (C) 1/4-in. thick with clear plexiglass walls. Bolts are placed at 1-1/2-in. intervals along the copper gasket to enable the system to be sealed.

The Coanda surface (D) was designed to provide a two-dimensional system and consists of three flat surfaces as shown in Figure 2. Two dimensional flow was obtained by using a channel width of 1/4 in. This system was chosen in order to obtain a configuration which was an intermediate one between a single flat plate and a round surface. A copper shroud (E) is included with spacers (F) of different lengths to allow the distance between the top of the Coanda surface and the shroud to be varied. The gap at the primary flow outlet is obtained by a copper regulating device (G) which enables the gap to be varied up to 1/4 in.

The primary stream is pumped through a small reservoir at the base of the Coanda surface and leaves through the gap. When the primary flow rate is raised to a minimum value, necessary for the Coanda effect to take place, the stream attaches itself completely to the Coanda surface and causes the entrainment of the secondary flow to begin. The primary and secondary streams combine along the nozzle surface and flow to the end of the channel where the solution is drawn off through a 2-in. copper pipe epoxied into the plexiglass side plate (H).

The fluid which makes up the primary stream is drawn off from the 2-in. pipe through a reducing tee and is pumped by a centrifugal pump (I), through a rotameter (J) and into the primary jet reservoir (K). The remaining fluid is returned to the storage reservoir through the 2-in. pipe. In order to measure the secondary flow rate a flexible hose is attached to the 2-in. return pipe and raised above the fluid level in the reservoir.

Pressure taps were incorporated along the Coanda surface at the center of each flat plate, at the top of the nozzle surface and along the downstream section of the nozzle. In all, six pressure taps were used. Six manometers were provided to measure the pressure profiles along the nozzle surface, for various gap and shroud settings, at different primary stream velocities. The manometer indicating fluid used was a Meriam blue fluid immiscible in water and having a specific gravity of 1.725.

Plastic polarizing plates, placed between glass plates to prevent them from bending, were held, crossed at 90° in a wooden support, and placed over the channel. The lighting consisted of a high intensity General Electric reflector bulb placed about 2 ft. from the polarizing plate to prevent heating of the plastic polarizing plates.

Copper cooling coils were placed inside the reservoir, and cold water was used as a coolant to prevent the solution from becoming heated by the high intensity lamp and the pump.

The Coanda nozzle described above was designed to facilitate the investigation of the effect that changing the parameters which govern the Coanda effect has on secondary flow entrainment and pressure profiles along the nozzle surface. Three parameters in particular were made variable; the primary jet outlet gap, the shroud distance and the primary jet flow rate.

The gap distance was set at three different values, 7/32, 7/64, and 7/128 in., and the shroud was set at 7/8, 11/8, and 19/8

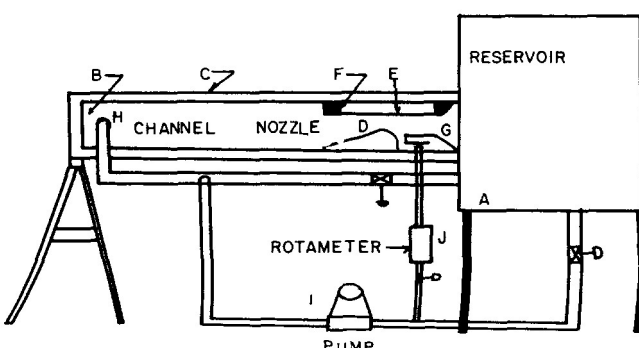


Fig. 1. Coanda effect flow visualization apparatus.

in., for each gap setting except the last where shroud distances of only 7/8 and 19/8 in. were used. For each combination of gap and shroud distance, several primary jet velocities were employed. For each primary velocity, the system was allowed to stabilize, and secondary flow and pressure measurements were taken.

The Coanda nozzle was assembled, sealed, and placed in the reservoir window. The flow rate was adjusted by a valve, located below the rotameter, and measurements were taken. The flow rate was then readjusted and the system was allowed to come to equilibrium again before the next set of measurements were made.

Photographs were taken to obtain a visual record of the effects of changing the geometrical parameters on the Coanda type flow, using the milling yellow dye solution for different gap and shroud settings.

## EXPERIMENTAL RESULTS

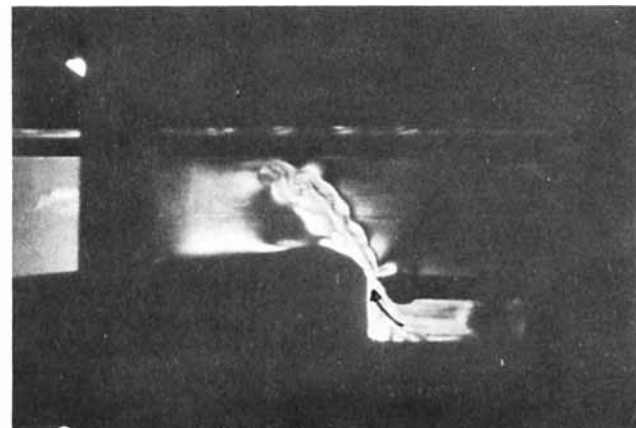
### Flow Visualization Observations

The flow visualization technique used to investigate the Coanda effect is based on the fact that certain substances become temporarily doubly refracting (anisotropic to the passage of light) when subjected to shearing stresses. When a doubly refracting substance is viewed by transmitting light between two polarizing plates, visible interference patterns which are related to the material dimensions, properties, and shearing stresses in the specimen are produced. A complete treatment of photoelastic theory is given by Frocht (6). Prados and Peebles (15) have developed an experimental technique for the determination of velocity distributions in two-dimensional laminar

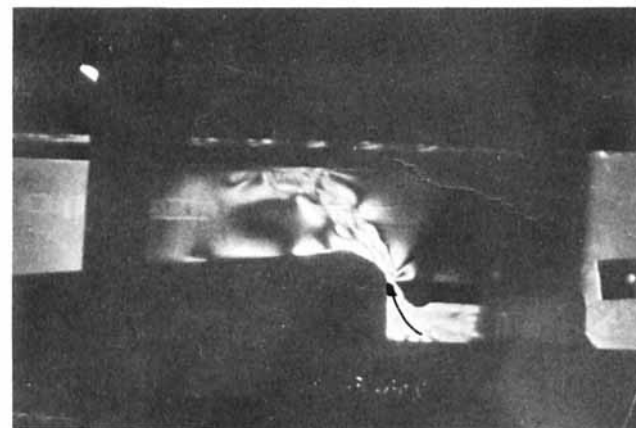
flow systems. The visible interference patterns that are observed through the polarizing plates are composed of light and dark bands, which appear stationary in laminar flow but take on a random eddying motion in turbulent flow. The amount of double refraction is a single-valued, increasing function of shear stress for a given doubly refracting liquid.

General knowledge of the flow field combined with high speed motion pictures and still photographs have been used in this study to determine a mechanism for flow attachment and entrainment of secondary fluid. Figures 3a to 3d are presented here to show the birefringent patterns obtained for various flows (that is, laminar and turbulent). A brief discussion of the interpretation of birefringent patterns follows. Figure 3a shows the system of a jet stream issuing next to a Coanda surface. The flow is from right to left. Light and dark wavy lines can be seen, indicating that the flow is in a transition region between pure laminar and turbulent flow. The fluid velocity is increased in Figure 3b and as expected the orderly pattern of light and dark lines, seen in Figure 3a, begins to break down becoming disorderly. Figures 3c and 3d show the system of a turbulent primary jet. In these cases the light and dark lines are reduced to light and dark patches randomly appearing and disappearing over the entire flow field.

The following are observations made from a careful examination of a high speed motion picture of the Coanda effect combined with pressure and flow measurements taken along the Coanda surface. In the first case the shroud was in the lowest position at a distance of  $\frac{7}{8}$  in. from the nozzle surface, and the gap is set at  $\frac{7}{32}$  in. Initially the primary jet attaches to the surface, but no secondary entrainment occurs. As the primary jet flow rate is increased,



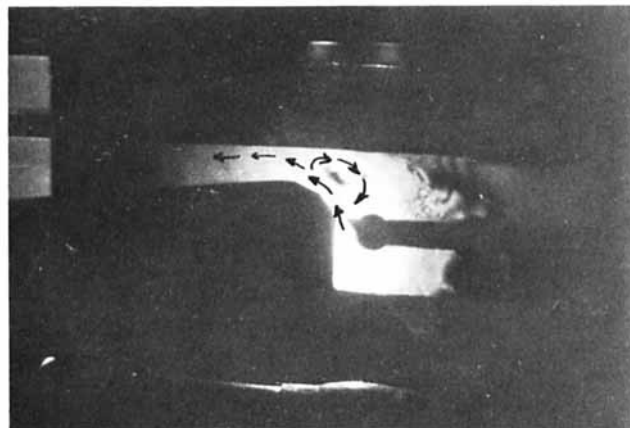
(a).



(b).



(c).



(d).

Fig. 3. Birefringent patterns for laminar and turbulent jets.

the jet becomes attached at farther distances along the Coanda surface and secondary flow begins. A large area of recirculating flow is noticeable in the intermediate and primary velocity ranges (see Figures 3d and 6). The recirculating flow region decreases with increasing primary flow rates until it disappears, because of the increased suction along the surface. This conclusion is drawn on the basis of observations of pressure profiles along the deflection surface at the conditions where the recirculating flow patterns are drawn toward the deflection surface. At this point the most effective stage of the Coanda phenomenon is present because the energy loss associated with the recirculating flow is no longer present. Secondary entrainment data verifies this in that the highest secondary entrainment occurs at these conditions.

In the second case the shroud is essentially removed, being located in its highest position, 19/8 in. above the Coanda surface. For this situation the primary jet detaches almost immediately from the Coanda surface, at the lower primary velocity ranges (see Figure 4a). In the intermediate primary velocity ranges, the jet becomes attached for a longer distance along the nozzle surface. After the point of detachment, part of the stream deflects off the top surface and begins to form a recirculating flow. At the higher primary velocities the stream attaches along the nozzle surface, but a large area of reversed circulation is created above the entire length of the nozzle, preventing significant entrainment of the secondary fluid (see Figure 4b).



Fig. 4a. Detachment of primary stream at low velocities.

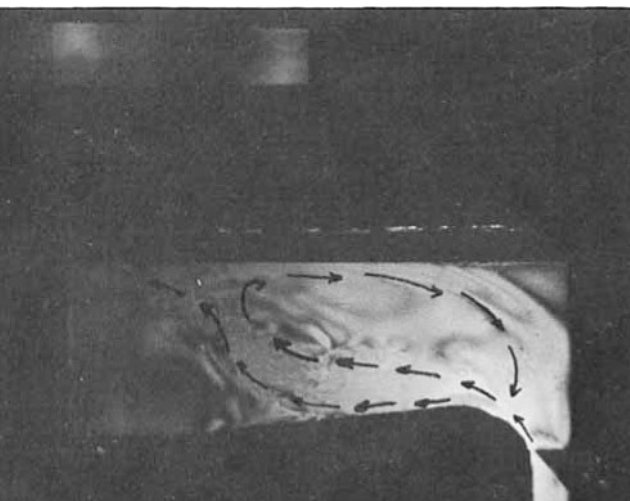


Fig. 4b. Attached primary flow accompanied by flow reversal above the Coanda surface.

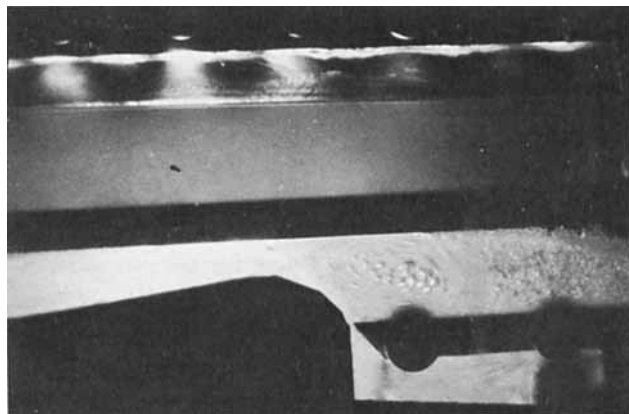


Fig. 5. Partial air entrainment showing reverse vortex established at intermediate primary velocities.

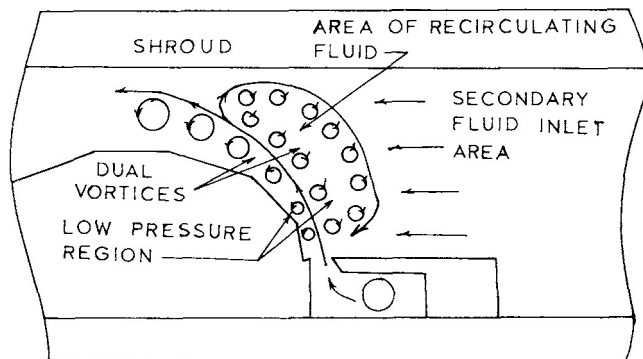


Fig. 6. Schematic of the mechanism governing the Coanda effect.

When air is used as the secondary fluid medium, the high degree of turbulence and mixing created by the Coanda effect becomes particularly evident in that the primary jet of milling yellow solution becomes completely aerated within a short contact time (see Figure 5).

#### Proposed Mechanism

The photographs shown in Figures 3 to 5 are representative of those used to determine the mechanism governing the Coanda type flow. In addition, quantitative flow data and pressure data have been analyzed in order to clarify certain aspects of the flow mechanism. A schematic diagram of the proposed model is shown in Figure 6 depicting the flow field obtained using an intermediate primary stream flow rate.

As the primary stream leaves the inlet reservoir through the gap, a jet consisting of double vortices is created (see Figure 6). This double vortex phenomenon had been reported previously by Miller (13) who used a milling yellow dye solution to investigate the properties of flow down a single step and a jet issuing from a slot. The vortices close to the nozzle surface rotate inward toward the surface while the vortices on the unbounded side of the jet turn outward. The vortices are confined to a narrow band of fluid comprising the primary jet. The low pressure associated with the vortices on the nozzle side of the jet tends to pull the entire jet towards the deflection surface, but as the primary jet proceeds along the nozzle surface it encounters an adverse or positive pressure region and becomes detached (see Figure 3a and 3b). As the jet becomes detached it strikes the shroud and divides into two separate portions (see Figure 3d). The internal part flows downstream through the nozzle while the unbounded part flows back toward the secondary flow inlet region. The unbounded vortices maintain part of their rotational

motion tending to flow back upstream, turning downward, creating a large area of reversed circulating flow in the secondary inlet region, preventing secondary entrainment. This phenomenon has been reported previously by Cooper and Marek (5) who carried out experiments to design a blue flame oil burner which would utilize the recirculating flow to provide more complete combustion of the oil.

When the primary jet velocity is increased, the rotational motion of the vortices also increases thereby decreasing the pressure along the nozzle surface still further. This provides a more favorable pressure gradient along the deflection surface enabling the jet to remain attached for longer distances along the surface of the nozzle. The motion pictures show that as the primary velocity is increased the area of recirculating flow is drawn toward the nozzle surface and secondary entrainment begins. At the highest velocities, the region of reversed flow is completely eliminated, the jet is completely attached to the nozzle surface and the suction pressure along the Coanda surface is at its lowest value providing the greatest amount of secondary entrainment. Mehus (11) indicated that the function of the shroud is to force the entrained fluid to flow along a path parallel to the primary flow and create an acceleration of the flow as it passes over the

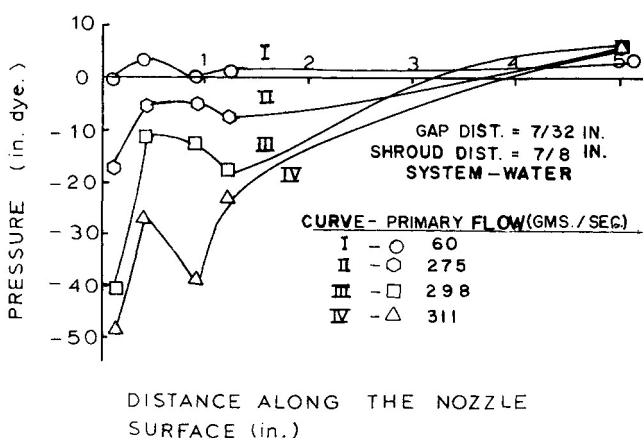


Fig. 7. Pressure profiles along the Coanda surface for varying primary flow rates.

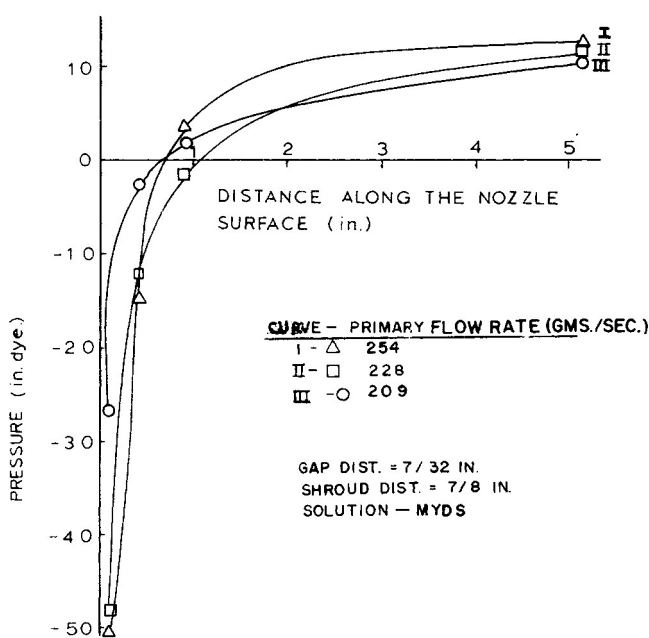


Fig. 8. Pressure profiles along the Coanda surface for varying primary flow rates.

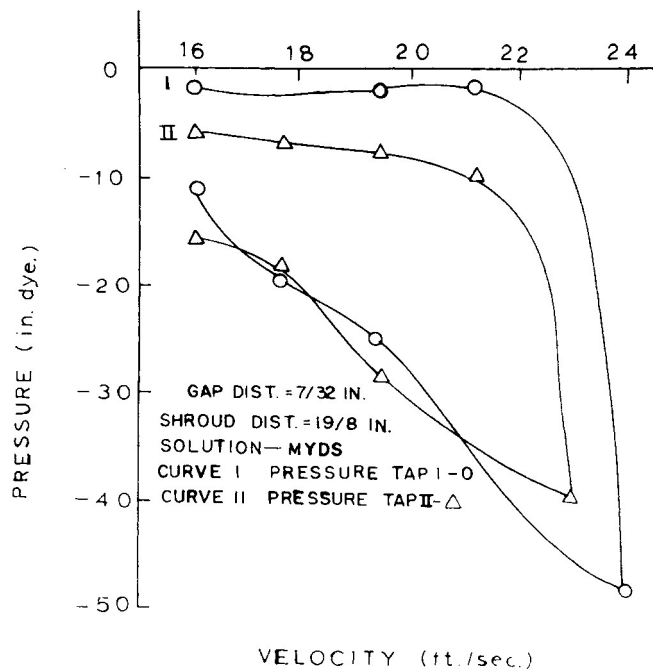


Fig. 9. Pressure hysteresis for increasing and decreasing primary velocities.

nozzle surface. With the shroud removed the guiding influence is no longer present and the large area of reversed flow is created (14).

The occurrence of the starting vortex had been reported previously by Reba (17) and Marwood (9), however the mechanism behind the creation of the recirculating flow in the nozzle secondary inlet region, its relation to the primary flow rate and pressure along the nozzle surface and its effect upon entrainment has not been reported to date.

#### Pressure Profiles and Flow Entrainment Data

Pressure profiles along the surface of the nozzle for water and myds are shown in Figures 7 and 8 respectively. Gauge pressures are plotted against position along the nozzle surface. For convenience the pressure units are expressed in terms of inches of indicator fluid. For each of the gap settings and shroud setting of 7/8 in., stable pressure profiles are obtained. These consist of a low pressure region followed by positive pressure which indicates detachment of the flow from the surface of the nozzle.

The effect of increasing the primary flow rate for a specific geometry can be seen in Figure 7. There is a significant increase in the suction pressure along the surface as the primary flow rate is increased. This indicates that the pumping power of a Coanda nozzle is more effective at higher primary flow rates because of this increase in suction pressure. This conclusion is verified by the entrainment data which shows higher secondary flow for higher primary flow rates. This effect also occurs for the other geometries as can be seen in Figure 8.

Previous investigators (3, 9) have indicated that the method of jet attachment initiation might have an effect on the properties of a Coanda type system. With the shroud placed in its lowest position this was not the case as evidenced by the fact that the pressure profiles were the same, whether approached from low or high primary flow rates. However, with the shroud in its highest position the method of flow initiation becomes important. This is shown in Figure 9. A substantially higher suction pressure is obtained at points along the surface after the flow has been

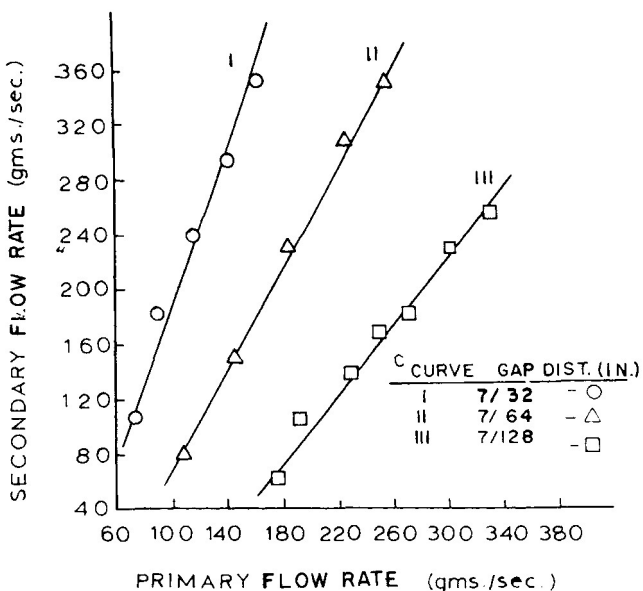


Fig. 10. Secondary flow rate versus primary flow rate different gap settings using water.

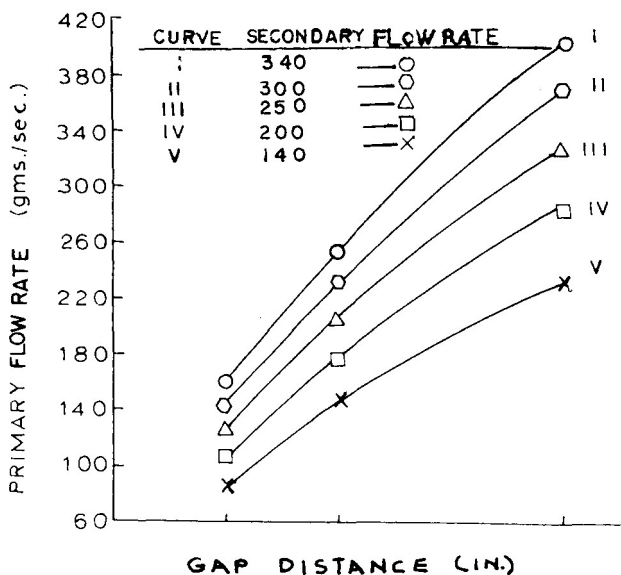


Fig. 11. Primary flow rate versus gap distance for different secondary flow rates using water.

fully attached, at the highest primary flow velocity, than those obtained by increasing the primary flow velocity. Figure 9 shows the change in pressure at two pressure taps along the deflection surface for increasing and then decreasing primary flow velocities. This shows that for this particular geometry a hysteresis effect becomes important in the process of flow attachment initiation.

The effect of varying the average primary flow rate on the secondary flow entrainment for a constant shroud distance of 7/8 in. and varying gap distance for water is shown in Figure 10. The data show that for a particular gap setting and shroud distance an increase in the primary flow rate results in higher entrainment rates. A minimum, critical primary flow rate is necessary to obtain the entrainment properties that accompany the Coanda type flow.

Cross plots of the primary velocity required to obtain a specific secondary flow rate of water at different gap distances are shown in Figure 11. Higher primary flow rates are required to obtain a specific secondary flow rate with increasing gap distance. The data shows that the optimum geometrical configuration occurs at the smallest gap setting employed.

The effect of viscosity and curvature on the pressure distributions and flow augmentation characteristics of the Coanda effect can be seen by comparing the data obtained using a multiple flat plate device and water with data obtained by von Glahn (22) and Marwood (9) whose apparatus consisted of a single flat plate as the deflection surface with air as the fluid used, and Roderick (19) who used a (circular) quadrant as the deflecting surface also with air.

Figure 12 shows pressure distributions for 4-in. circular quadrant (curve 1) using a nozzle diameter of 1/16 in. and a single flat plate (curve 2). A significant difference can be seen between the pressure profiles presented by Roderick (19) (curve 1) and those obtained by von Glahn (22) (curve 2, Figure 12), and the data presented in Figures 7 and 8. With a curved surface the suction pressure region extends over a longer distance along the quadrant than when a flat plate is used. This indicates that a sharp corner tends to induce flow detachment. With a single flat plate device the suction pressure is much stronger initially than the pressure obtained with a quadrant but rapidly becomes positive indicating flow detachment.

The effect of viscosity at both low and high shear rates (that is, low and high primary velocities) on the secondary flow entrainment properties of a Coanda nozzle can be seen dramatically by comparing the data obtained using water with a multiple flat plate device with data obtained by Marwood for a single flat plate device using air.

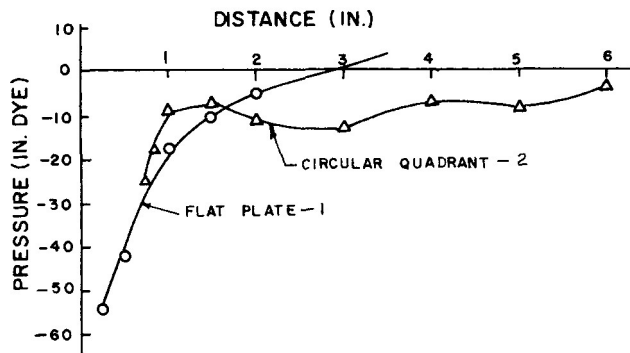


Fig. 12. Representative pressure profiles for a circular quadrant and a single flat plate using air.

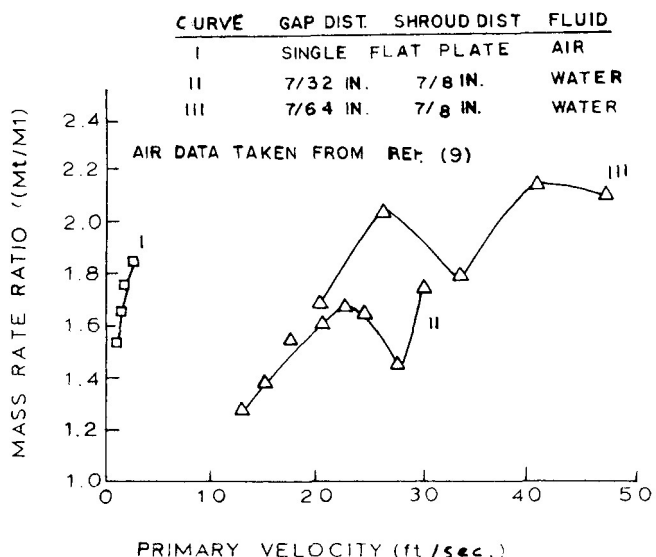


Fig. 13. Mass rate ratio versus linear primary velocity for different geometries and fluids.

Graphs of the mass rate ratio, which provides a measure of the ability of the Coanda device to entrain secondary fluid, versus the primary flow velocity required to obtain the secondary flow are presented in Figure 13 for air and water. For a particular mass rate ratio the primary velocity required to obtain that ratio is a factor of 10 higher for the liquid cases compared to the air case. In fact, the Coanda phenomenon is unobtainable with the liquids when the primary velocities are in the same range as those used in the experiments with air made by Marwood.

## CONCLUSIONS

At low primary flow rates there is no secondary flow entrainment and only partial adherence of the primary jet to the nozzle surface. With increasing primary flow a large area of reversed recirculating flow is created at the top of the Coanda surface, and again no secondary flow is obtainable. As the primary flow rate is increased further, the reversed flow is pulled close to the nozzle surface and secondary entrainment begins. The primary stream becomes completely attached to the surface and a turbulent mixing zone is created. The photographs showed that a well defined mixing region is established along the nozzle surface (see Figure 4b).

With the shroud removed the primary stream becomes attached to the surface only at high primary rates, but no secondary entrainment occurs. The reason for this can be seen in a large area of reversed flow above the entire length of the Coanda deflection surface. The purpose of the shroud is to guide the streamlines of the entrained flow in a direction parallel to the surface of the nozzle, enhancing the suction pressure. Comparing the pressure profiles obtained both with the shroud in place and removed shows that this is indeed the case.

Pressure profiles measured along the surface of the nozzle for different geometries show that a region of low (suction) pressure exists along the initial part of the nozzle with a positive pressure region following it. This phenomenon has been reported previously for air systems, but no data on liquid systems has been presented. Increases in the primary flow rate result in significantly larger suction pressures along the nozzle, indicating that greater secondary entrainment should occur. By comparing the graphs of pressure profiles for the various primary flow rates and those of secondary entrainment rates, corresponding to primary flow rates, we can see that increasing suction pressure does indeed increase the amount of secondary flow.

Increasing the primary velocity increases the amount of secondary entrainment when air is the fluid medium; however, no data has been reported to date to show the relationship of secondary entrainment to pressure profiles and primary flow rates for either air or liquid systems.

The method of flow attachment is important in the case where the shroud is removed. Higher suction pressures are obtained after the flow has been fully attached upon decreasing the primary jet velocity than when the primary flow rate is initially increased.

For a constant shroud distance, with the shroud in its lowest position, increasing the gap distance decreases the pumping ability of the nozzle when water is used, in that a higher primary flow rate is required to obtain a specific secondary flow rate.

For water systems and air systems, increasing the primary jet velocity increases the amount of secondary entrainment for a particular geometrical configuration, which is to be expected, since the suction pressure increases with

primary velocity for a fixed set of parameters within the nozzle.

A comparison is made of the pressure profiles obtained with smoothly curved deflection surfaces using air and those obtained with a single plate deflection surface. The suction pressures are maintained along the entire length of the deflection surface when a curved surface is used, while the flat plate devices show a sharp increase in the pressure leading to a region of positive pressure, at short distances along the surface. This indicates that flow detachment is induced by a sharp corner on the deflection surface.

The results of the experimental study presented here do not establish the direction of the velocity gradient at the Coanda surface and the local velocity in a flowing fluid. These measurements need to be made to further elucidate the mechanism governing the Coanda type flow and to provide design information necessary for the intelligent application of the effect.

## ACKNOWLEDGMENT

This study was supported in part by the Chicago Bridge and Iron Company. We also wish to acknowledge several helpful discussions that we have had with Messers T. Delahunt, R. Laverman and D. Matschke. In addition we wish to express our appreciation to Dr. Coanda who contributed many helpful insights to this work.

## LITERATURE CITED

1. Bailey, A. B., *NASA Tech. note, TN 4272*, 49 (Aug., 1961).
2. Block, R., and M. Reiner, *Bull. Res. Council Israel*, **2**, 263 (1952).
3. Bourgue, C., and B. G. Newman, *Aeron. Quarterly*, **11**, 201 (1960).
4. Boyer, L. J., *USAAF Tech. Report F-TR-2144ND* (1946).
5. Cooper, D. W., and C. J. Marek, *IITRI Report to Am. Petrol. Inst.*, Div. Marketing, 1723A (Jan., 1965).
6. Frocht, M. M., "Photoelasticity," Vol. 1, Wiley (1941).
7. Keller, T. B., *J. of Appl. Physics*, **28**, 829 (1957).
8. Korbacher, F. K., *Canadian Aeron. Inst.*, **8**, 1 (1962).
9. Marwood, R. M., M.S. thesis, Purdue Univ., Lafayette, Ind. (1948).
10. McArdle, J. G., *NACA Tech note, TN 4264* (1958).
11. Mehus, J., *UTIAS, Tech. Note*, 79 (Jan., 1965).
12. Metral, A. R., Headquarters, Air Material Command, *Wright Field Report F-TS-823Re* (1939).
13. Miller, E. B., Wyle Laboratories, *NASA Report CR-88-703* (1967).
14. Panitz, T., M.S. thesis, Ill. Inst. Technol., Chicago (1970).
15. Prados, J. W., and F. N. Peebles, *AIChE J.*, **2**, 225 (1959).
16. Prandtl, L., "Aerodynamics Theory," W. T. Durand, ed., **3**, 128 (1930).
17. Reba, Imants, *Sci. American*, **214**, 84 (1966).
18. Reiner, Marcus, *Physics Today*, **9**, 16 (1956).
19. Roderick, W. E. B., *UTIA Tech. Note 51*, Inst. Aerophysics, Univ. Toronto, Canada (1961).
20. Schlichting, M., "Boundary Layer Theory," Pergamon, 496 (1955).
21. Torda, T. P., K. N. Ghia, and E. L. Victory, *J. Appl. Mech.*, **4**, 553 (1968).
22. Van Glahn, U. H., *NACA Tech. Note TN 4272*, (June, 1958).
23. Victory, E. L., Huyck Corp. Research Center, Contract AF-33 (657)-11697 (Oct., 1969).
24. Voedisch, A., *Wright Field Report F-TR-2155ND* (1947).
25. Von Karman, Theodor, in *Appl. Mech., Reissner Anniv.* Vol., 461 (1949).
26. Yen, K. T., Dept. Aero. Eng., Rensselaer Polytechnic Inst., Contract A.F. 18 (600)-992 (1955).

*Manuscript received January 20, 1971; revision received June 16, 1971; paper accepted June 17, 1971.*